SIMULATION OF FLUID POUND EFFECTS ON THE ROD STRING

Ferhat Yavuz, Dr. James F. Lea, Dr. James Cox, Divyakumar Garg and O. Fasokun
Texas Tech University

ABSTRACT
Using adiabatic compression of gas in the pump, a model is shown that can be used to calculate the down-hole pump dynamometer card for various degrees of pump fill of liquids and gas at various degrees of pressure. The load release portion of the card is emphasized. It is shown how the lower pressure gas in the pump promotes what is commonly termed fluid pound or slap and higher pressure gas in the pump promotes what is termed gas interference. The equations that are needed to model these effects for inclusion into wave equation pump models are presented and example calculated pump cards are shown, calculated from wave equation simulations. Since even with so-called fluid pound, gas is first compressed before the plunger encounters the mostly incompressible fluid in the pump, the traveling valve always encounters compressed gas sufficient to open the valve before the plunger "hits" the fluid. This is true as long as gas is in the barrel when incomplete fluid fill occurs. Given this fact, the time step in wave equation solution is examined as the load release in the so called "fluid pound" can happen over a very short time and longer time steps in the wave equation simulation could mask forces from short term forces. The effects of load release on forces in the rods are studied with various conditions of incomplete fill of the pump, and low intake pressure. Other parameters such as pump fillage, intake pressure and sinker bars are examined for their effects on calculated rod compression.

INTRODUCTION

Fluid pound is associated with incomplete fillage of the downhole pump. There is considerable opinion that the pound and associated possible damage is related to the pump traveling through gas and then striking or “pounding” the fluid when it is encountered by the pump traveling downward. However in this discussion it is shown that severe rod compression can be encountered when no impact force is simulated of the pump “striking” the fluid level. Instead it appears that with incomplete pump fill and low pump intake pressure, the pump decelerates as gas in the barrel is compressed leading to a “stacking” effect in the rods up from the pump, leading to severe rod compression. Some examples of what can mediate this effect are presented as well.

- “ The dynamic loads during fluid pounding can cause several detrimental effects on the downhole equipment.: The rod string can experience buckling that leads to rod breaks,; rod-to-tubing wear is increased; shock loads contribute to coupling failure due to unscrewing; and pump parts can be damaged (as well as tubing), if unanchored. On the surface, shock loads can damage pumping unit bearings, and can lead to instantaneous torques that overloads the speed reducer. “ *(Takacs[23])*

Fluid pound is usually said to be the result of the pump traveling through the gas filled portion of the pump and then “hitting” the fluid. This then is said to put compression into the rods and to cause damage to the rod string, etc. However if you view Figure 1, the first type of so-called pump card is the type of card that is normally seen for fluid pound. In the first type of card shown in Figure 1, there is not compression shown. This is the typical pump card that is seen for the situation of so-call fluid pound or rapid load release when the intake pressure is low.
The second type of card shown in Figure 1, shows that some compression is evident from presumably fluid pound. This type of bottom hole card is not typical. Is it possible that fluid pound does not in general lead to compression or buckling in the lower rods?

Even in fluid pound, there is gas compression. Assume 100” bottom hole stroke. Assume ½ of the bottom hole stroke is filled with fluid and the other half with gas at 100 psi. Assume 2000 psi over the TV. Then:

P1/P2 = 100/2000 = V2/V1 = (X x A) / (50” x A) =
Solve for X and it’s equal to 2.5 inches or the TV will open when the TV is 2 ½” from the fluid.

If the initial pressure in the barrel is 50 psi, then the TV opens when the TV is 1 ¼” from the fluid. For lower intake pressures it is seen that the traveling valve opens when the pump is very close to the fluid level in the pump barrel.

So the TV always opens due to gas compression before it hits the fluid. It would never hit the fluid without gas having enough pressure to open the TV first. Still the plunger hits the fluid with the TV open and goes from travel in the gas to impacting the fluid and traveling downward through the fluid column.

Also what about when the pump is full of fluid? The load release happens quickly but no compression or fluid pound is reported. This is presumed to be because the pump is traveling very slowly compared to mid-stroke.

In Figure 2, fluid pound is usually shown in "cartoon" fashion as showing no unusual compression as a result of fluid pound, although usually in the text describing fluid pound, it usually says rod compression is a result of fluid pound. The cartoon in the Figure 2 is showing what is typical of pumps cards in the industry to identify fluid pound. But again where is the compression? If compression is in the rods, it is not in the rods just above the pump according to these types of cards as in Figure 2.

However in the Figure 3, compression is shown for a fluid pound card. This would show compression due to fluid pound, although this type of bottom hole card is usually not shown with a fluid pound situation. Usually the downward spike, indicating compression to the rods over the pump, is not present. Also in this pump card there is a downward spike earlier in the stroke and it is possible both spikes are due to something other than fluid pound, such as solids in the pump.

ANALYSIS

Before considering the rod boundary condition for the rods above the pump, equations for the complete wave equation analysis are presented below. These equations are somewhat unique as it shows a way to establish boundary conditions at rod junctures where tapered rods are connected without having to average the rod properties and sizes in the equations of motion. Equations are shown for both the so-called predictive and diagnostic type of wave equation beam pump computer models.

The equation of motion, Equation (1), for the constant property sucker rod string is presented in several references (1, 4,5,13, etc.) which includes viscous dampening.

$$\frac{\partial^2 U}{\partial t^2} = \frac{Eg}{\rho}\frac{\partial^2 U}{\partial x^2} - \frac{c\pi}{2L}\sqrt{\frac{Eg}{\rho}}\frac{\partial U}{\partial t} \quad \text{..(1)}$$

For changing rod properties with depth (tapered string) the above equation can be written as Equation (2):

$$\frac{\partial^2 U}{\partial t^2} = \frac{g}{\rho A}\frac{\partial}{\partial x}\left[EA\frac{\partial U}{\partial X}\right] - CV\frac{\partial U}{\partial t} \quad \text{...(2)} \quad \text{where}: C = \frac{c\pi}{2L} \text{ and}$$

V is the speed of sound in the rod material.

If the following development, only Equation (1) is used but a method of analysis for a tapered rod string is still developed below. The below force equation is or can be at a rod taper where properties and cross section change. There can be a Δx in the rod a, and a Δx in the rod at b of different lengths.

$$F_a = F_b \text{.......}$$

Or:

$$(AE)_a\left(\frac{\partial U}{\partial x}\right)_{ia} = (AE)_b\left(\frac{\partial U}{\partial x}\right)_{ib} \quad \text{...(4)}$$

Following a procedure in Reference 20 and expanding Ui+1 and Ui-1 about Ui gives in Equations 5a and 5b:

$$U_{i-1} = U_i - \left(\frac{\partial U}{\partial x}\right)_{ia} \Delta X_a + \left(\frac{\partial^2 U}{\partial x^2}\right)_{ia} \frac{(\Delta X_a)^2}{2} \text{...}(5a)$$

$$U_{i+1} = U_i - \left(\frac{\partial U}{\partial x}\right)_{ib} \Delta X_b + \left(\frac{\partial^2 U}{\partial x^2}\right)_{ib} \frac{(\Delta X_b)^2}{2} \text{..}(5b)$$

Solving Equations 5a and 5b for the force at i gives:

$$F_{ia} = (AE)_a \left(\frac{\partial U}{\partial x}\right)_{ia} = \left(\frac{\partial^2 U}{\partial x^2}\right)_{ia} \left(\frac{\Delta X_a}{2}\right)(AE)_a + \left(\frac{U_i - U_{i-1}}{\Delta X_a}\right)(AE)_a \text{............}(6a)$$

$$F_{ib} = (AE)_b \left(\frac{\partial U}{\partial x}\right)_{ib} = \left(\frac{\partial^2 U}{\partial x^2}\right)_{ib} \left(\frac{\Delta X_b}{2}\right)(AE)_b + \left(\frac{U_{i+1} - U_i}{\Delta X_b}\right)(AE)_b \text{..............}(6b)$$

All U's are at time j in Equations 5 and 6. Representing the time derivatives with finite difference expressions for rods a and rods b in Equation (1) gives:

$$\left(\frac{\partial^2 U}{\partial x^2}\right)_{ia} = \frac{U_{i,j+1} - 2U_{i,j} + U_{i,j-1}}{(V_a \Delta t)^2} + \left(\frac{c}{V_a \Delta t}\right)(U_{i,j+1} - U_{i,j}) \text{............................}(7a)$$

$$\left(\frac{\partial^2 U}{\partial x^2}\right)_{ib} = \frac{U_{i,j+1} - 2U_{i,j} + U_{i,j-1}}{(V_b \Delta t)^2} + \left(\frac{c}{V_b \Delta t}\right)(U_{i,j+1} - U_{i,j}) \text{............................}(7b)$$

Where j and i index time and distance. Equating (6a) and (6b) and substituting for the second derivative of U with respect to x from Equations (7) gives:

$$\begin{aligned} &\alpha_a\left(U_{i,j+1} - 2U_{i,j} + U_{i,j-1}\right) + \beta_a\left(U_{i,j+1} - U_{i,j}\right) + \gamma_a\left(U_{i,j} - U_{i-1,j}\right) \\ &= \alpha_b\left(U_{i,j+1} - 2U_{i,j} + U_{i,j-1}\right) - \beta_b\left(U_{i,j+1} - U_{i,j}\right) + \gamma_b\left(U_{i+1,j} - U_{i,j}\right) \text{......................}(8) \end{aligned}$$

$$where: \alpha = \frac{\Delta XAE}{2(V\Delta t)^2}, \text{.............} \beta = \frac{\Delta XAEC}{2V\Delta t}, \text{..............} \gamma = \frac{AE}{\Delta X}$$

In Equation (8) all the groupings are either groups of a or b properties. No averaging of properties is required as the calculation proceeds from a to b. Also the x increments can be equal or unequal across the boundary (i.e. as from a one rod to a different rod).
Solving for Ui, j+1 gives an algorithm for the "design" or predictive type of analysis:

$$U_{i,j+1} = \frac{U_{i,j}\left(2\alpha_s + \beta_s - \gamma_b - \gamma_a\right) - \left(U_{i,j-1}\right)\left(\alpha_s\right) + U_{i+1,j}\left(\gamma_b\right) + U_{i-1,j}\left(\gamma_a\right)}{\left(\alpha_s + \beta_s\right)} \text{............}(9)$$

$$where:$$
$$\alpha_s = \alpha_a + \alpha_b$$
$$\beta_s = \beta_a + \beta_b$$

The technique of solution of the predictive problem is covered elsewhere [4, 7, 13, 14].
The solution involves evaluating the rod wave equation over the complete length of the rod string for each time in a complete pump cycle. The surface motion is supplied at each time by a geometric formula [9, 10]. At each time, a pump boundary condition that specifies pump loading is used. The solution requires repetitive complete cycles until the solution has converged usually requiring at least 2-4 cycles.

The stability of the solution is affected by the choice of the time increment. For a constant x increment, the solution is stable[13] for $\Delta t \leq \Delta x/V$ where Δt is the smallest value for any segment.

Another type of rod pump analysis is to input a dynamometer card as points of load and position at the surface and calculate down the rod string to just above the pump. This is referred to as the "diagnostic" problem. Instead of using a Fourier series solution[4] to develop the diagnostic type of beam pump analysis, Equation (8) is solved for U i+1, j.

$$U_{i+1,j} = U_{i,j+1}\left(\frac{\alpha_s+\beta_s}{\gamma_b}\right) + U_{i,j-1}\frac{\alpha_s}{\gamma_b} - U_{i-1,j}\frac{\gamma_a}{\gamma_b} - U_{i,j}\left(\frac{2\alpha_s+\beta_s-\gamma_b-\gamma_a}{\gamma_b}\right) \text{.........(10)}$$

For the rod boundary condition above the pump when the load is released for the condition of partial pump fillage, the nomenclature and equations used are identified in Figure 4. Essentially as the pressure increases in the gas below the TV as the pump goes downward, the equations adiabatic compression are used. So the pressure at any location is found from:

$$P_2 = \{(P_1 V_1^k)/V_2^k\}^{1/k}$$

Where:
k is the ratio of specific heats for natural gas
V_1 is the initial volume of gas in the pump before the downstroke starts.
V_2 is the compressed volume of gas at any downward location of the pump
P_2 is the pressure in the gas as it is compressed

The use of this equation interfacing with the stress in the rods above the pump is, again, shown in Figure 4.

RESULTS OF FLUID POUND SIMULATIONS

Before simulations are shown, the forces required to buckle rods are shown in Figure 5. Note that the loads are small that cause buckling and for most rods the load is below 100 lbfs.

Simulations of fluid pound situations are then presented. Figure 6a and 6b show the base case of 60% pump fill, intake pressure of 30 psig, fluid gravity of 1.0, pump size of 1 ¾", spm=8, 144" surface stroke, conventional unit pumping clockwise. The rod string is an 86 tapered grade D rod string.

In Figure 6a, the predicted surface and pump cards are presented. In Figure 6b, the rod loads vs. depth are presented. The effective loads being negative are an indication of buckling if the load exceeds the buckling limit. A discussion of true forces and effective forces is presented in Reference 21. For this simulation a section of negative loading is shown in the rod string. This is the dotted line on the left. In fact very serious loading is indicated showing compression many times what would be required to buckle the rods. This shows that fluid pound (Figures 6 are for low intake pressure and the load release is rapid showing a so-called fluid pound situation) has apparently caused rod compression but there is no compression right above the pump. Most programs input some default value of pump resistance such as 100 lbfs to indicate flow through the TV and friction of the plunger through the barrel. However here it is not done to emphasize the other loading shown.

This downstroke compression is NOT due to the plunger “hitting” the fluid level. And again, no compression in the rods is shown above the pump. So why is there compression in the rod string in the fluid pound situation? It seems to be that when the gas in the barrel is compressed with incomplete pump fill and low intake pressures, the pump plunger decelerates and the rods above experience a “stacking” effect leading to severe compression in rods well above the pump. Again no upward compressive forces are input into this simulation.

To further investigate, in Figures 7, the intake pressure is varied from 50 psig to 110 psig. Note that the rod compression gradually diminishes to zero as the intake pressure is simulated to increase.

To investigate further, in Figures 8, the effects of pump fill are examined from 50 to 90% pump fillage with all at 7 spm. Note that the effects of fillage for these simulations have little effect. Normally it is said that the maximum velocity is near the center of the downstroke and if the fluid level is at this location, then more damage can result. However the simulations show that the effects of fillage are random and rod compression seems somewhat independent of the pump fillage. This may be because the pump velocity is not sinusoidal but is more erratic and the maximum in velocity at the pump is not in general at the center of the downstroke at the pump. However it is found that as the plunger nears the fluid level the pump slows it downward travel. Figure 9 shows the erratic nature of the pump velocity possible in a pump cycle.

Figure 10 shows the effects on the calculated compression force with adding sinker bars. Note that, at least in this case, the addition of sinker bars had little effect on the compression in the rod string.

CONCLUSIONS

Rod compression from fluid pound may not be due from the plunger hitting the fluid level. Substantial compression is simulated without this effect. The “hitting” effect may or may not add substantial compression in the rods but is thought to be a much smaller effect than what is simulated here.
The effect of the intake pressure on the rod compression is substantial.
The variation of the % pump fillage on rod compression seems to be less predictable.
Sinker bars may not eliminate the compression from so-called fluid pound.
You cannot see the magnitude of rod compression in the rod string from examining the pump card.
You should simulate pumping conditions with a wave equation predictive to see if you are in a damaging pumping condition that may be causing rod damage with a program that plots or indicate rod loading with depths.
Loading at only node points is not sufficient to see this type of loading.
It seems that the plunger slows as low pressure gas is compressed with incomplete pump fill and this deceleration of the plunger leads to a “stacking effect” in the rods up hole leading to severe compression in many cases examined.

NOMENCLATURE

A = Rod cross section area, ft^2 [m^2]
c = Input dampening factor, dimensionless
C = Dampening factor grouping, $\frac{c\pi}{2L}, \frac{1}{ft}, \left[\frac{1}{m}\right]$
E = Modulus of elasticity (of sucker rods), $\frac{lbf}{ft^2}\left[\frac{Pa}{m^2}\right]$
F = Force internal to rods due to dynamic stretch, lbf [Pa]
G= 32.17 $\frac{lbm}{lbf}\frac{ft}{\sec^2}, \left[\frac{kg-m}{N-\sec^2}\right]$
L = Length of rod string, ft [m]

S = Time, sec [S]
Δt = Increment of time, sec [S]

U = Dynamic rod displacement as a function, x and time, t, ft [m]
X = Downward positive location from the surface to a position on the rod string, ft [m]
ΔX = Increment of position, ft [m]
ρ = Density if rod materials, $\frac{lbm}{ft^3}\left[\frac{kg}{m^3}\right]$
V = Velocity sound in rods, $\frac{\text{ft}}{\text{sec}}\left[\frac{m}{S}\right]$
α, β, γ = Groupings of terms, Equation (8), $\frac{\text{lbf}}{\text{ft}},\left[\frac{Pa}{m}\right]$

Subscripts:
a - Signifies rod properties for “a” rods
b - Signifies rod properties for “b” rods
i - Index for distance, x
j - Index for time, t
s - Indicates sum of groupings

REFERENCES

1. Lea, J. F.: “Boundary Conditions used with Dynamic Models of Beam Pump Performance” presented at the Southwestern Petroleum Short Course, Lubbock, TX, April, 1988, p 251-263.
2. Gilbert, W. E.: "An Oil Well Pump Dynagraph," API Drilling and Production Practice, 1936, pp. 94-115.
3. Gibbs, S. G.: "Computing Gearbox Torque and Motor Loading for Beam Units with Consideration of Inertia Effects," Journal of Petroleum Technology (September 1975), pp. 1153-1159.
4. Gibbs, S. G.: "A General Method for Predicting Rod Pumping System Performance," paper SPE 6850 presented at the 1977 Annual Technical Conference and Exhibition, Denver, October 9-12.
5. Gibbs, S. G. and Neely, A. B.: "Computer Diagnosis of Downhole Conditions in Sucker Rod Pumping Wells," Journal of Petroleum Technology, (January 1966), pp. 91-98; Transactions, AIME, 237.
6. Gibbs, S. G.: "A Method of Determining Sucker Rod Performance: U.S. Patent No. 3,343,409 (September 26, 1967).
7. Gibbs, S. G.: "Predicting the Behavior of Sucker Rod Pumping Systems," Journal of Petroleum Technology (July 1963), pp. 769-778; Transactions, AIME, 228.
8. Gibbs, S. G.: "Computing Gearbox Torque and Motor Loading for Ultra High Slip Prime Movers," SPE 5149, presented at the 49th Annual SPE Conf. in Houston, TX, Oct. 6-9, 1974.
9. Gray. H. E.: "Kinematics of Oilwell Pumping Units," paper presented Amarillo, Texas, at the API Mid-continent District Meeting, March 27-29, 1963.
10. Svinos, J. G.: "Exact Kinematic Analysis of Pumping Units," paper SPE 12201 presented at the 1983 SPE Annual Technical Conference and Exhibition, San Francisco, October 5-8.
11. "API Catalog of Analog Computer Dynamometer Cards," API Bulletin llL2, First Edition, Washington, D.C., (1969).
12. "Design Calculations for Sucker Rod Pumping Systems," API Bulletin IIL, Third Edition, Washington, D.C., 1977.
13. Knapp, R. M.: "A Dynamic Investigation of Sucker Rod Pumping, "M.S. Thesis, University of Kansas, Topeka, Kansas (1969).
14. Doty, D. R. and Schmidt, Z.: "An Improved Model for Sucker Rod Pumping," SPE Engineers Journal, February 1983, pp. 33-40.
15. Nicol, T. H.: "Dynamic Analysis of Sucker Rod Pumping," M.S. Thesis, University of Oklahoma, Norman, OK (1982).
16. Chacin, J. E.: "Diagnostic and Design Techniques in Oil Well Pumping," PhD Thesis, University of Oklahoma, Norman, Oklahoma, 1986.
17. Schafer, Donald J.: "An Investigation of Analytical and Numerical Sucker Rod Pumping Mathematical Models," M.S. Thesis, Texas A&M University, College Station, Texas, (1987).

18. Chacin, U. and Purcupile, J. C., "A New Model for Studying Oilwell Pumping Installations, SPE 16918, presented at the 62nd Annual SPE Conf., Sept. 27-30, 1987.
19. Schafer, D. J., and Jennings, J. W., "An Investigation of Analytical and Numerical Sucker Rod Pumping Mathematical Models," SPE 16919, presented at the 62nd Annual SPE Conf., Sept. 27-30, 1987.
20. Carnahan, B., Luther, H. A., and Wilkes, J. O., Applied Numerical Methods, Wiley, 1969; p. 463.
21. Newman, K., Bhalla, K., "The Effective Force", CTES L.C., Conroe, TX. Technical Nole, Jan 13, 1999
22. Eickmeier, J. R., "Applications of the Delta II Dynamometer Technique", 17th Annual Technical Meeting. The Petroleum Society of C.I.M., Calgary, May, 1994
23. Takacs, G., Sucker-Rod Pumping Manual, Pennwell, © 2003
24. Rourk, R. J., and Young, W. C., *Formulas for Stress and Strain*, McGraw-Hill, NY,NY, 1982, P. 539

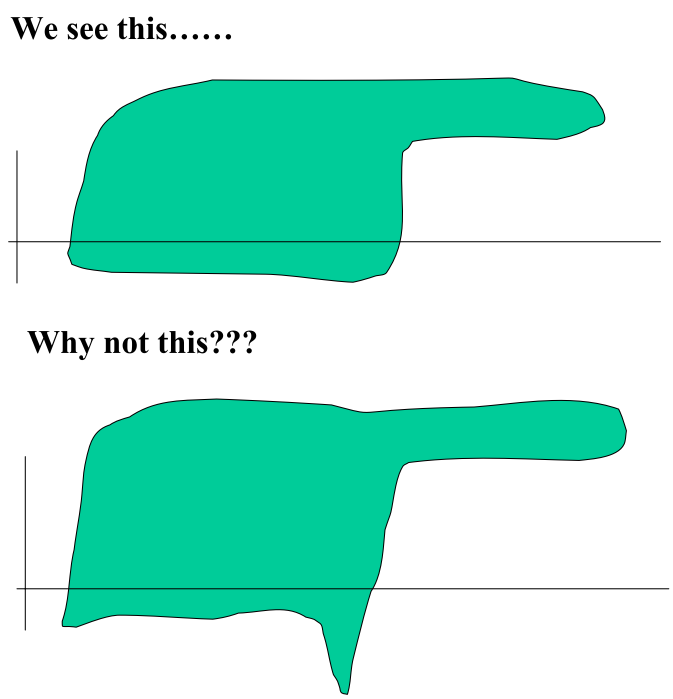

Figure 1 - Calculated (or Measured) Fluid Pound Dynamometer Cards in the Rods Over The Pump

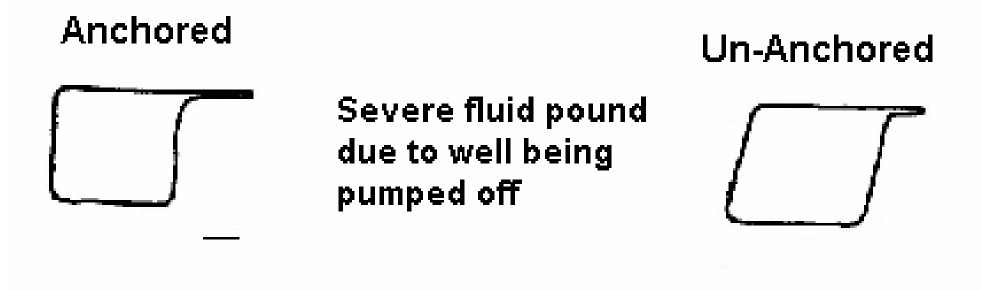

Figure 2 - Cartoon Representation of Fluid Pound Pump Cards

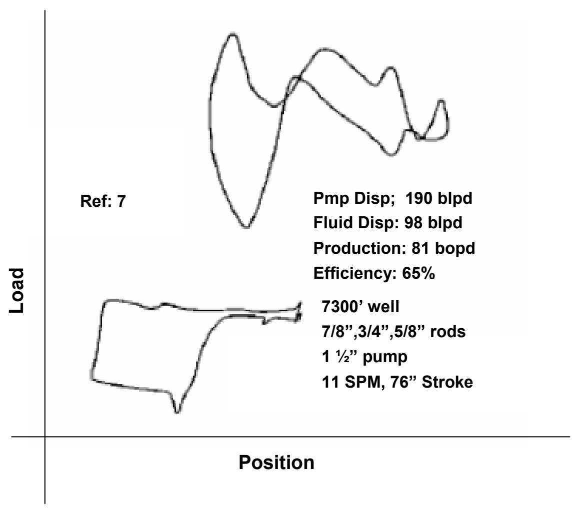

Figure 3 - Measure/Calculated Surface/Bottom Hole Cards Showing
Some Non-Typical Compression on Due to Fluid Pound

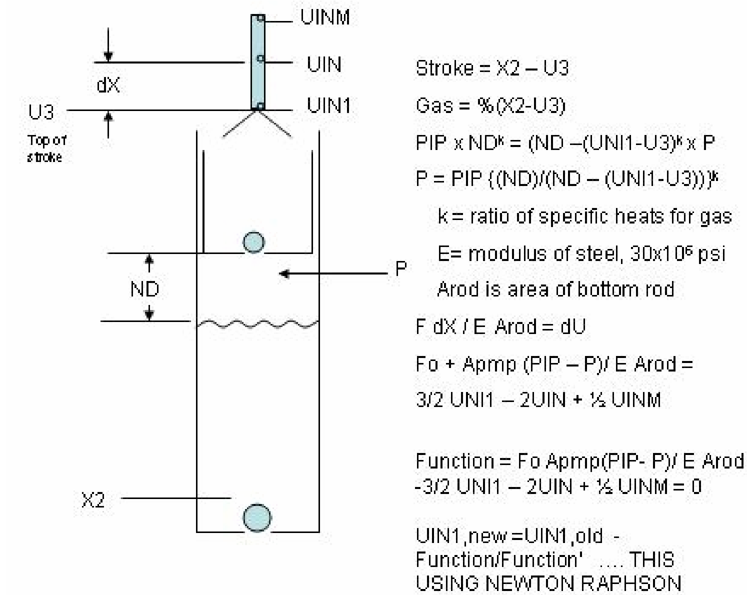

Figure 4 - Description of Terminology of Calculating Rod Loading
Above the Pump for Partially Filled Pump

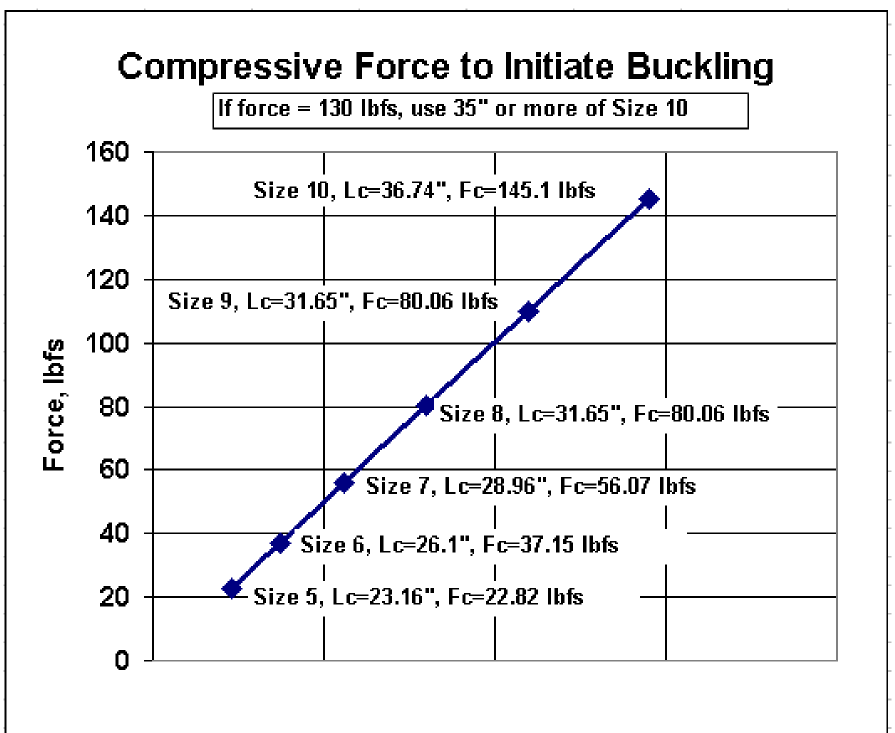

Figure 5 - Loads Predicted to Buckle Sucker Rods Of Various Sizes[24]

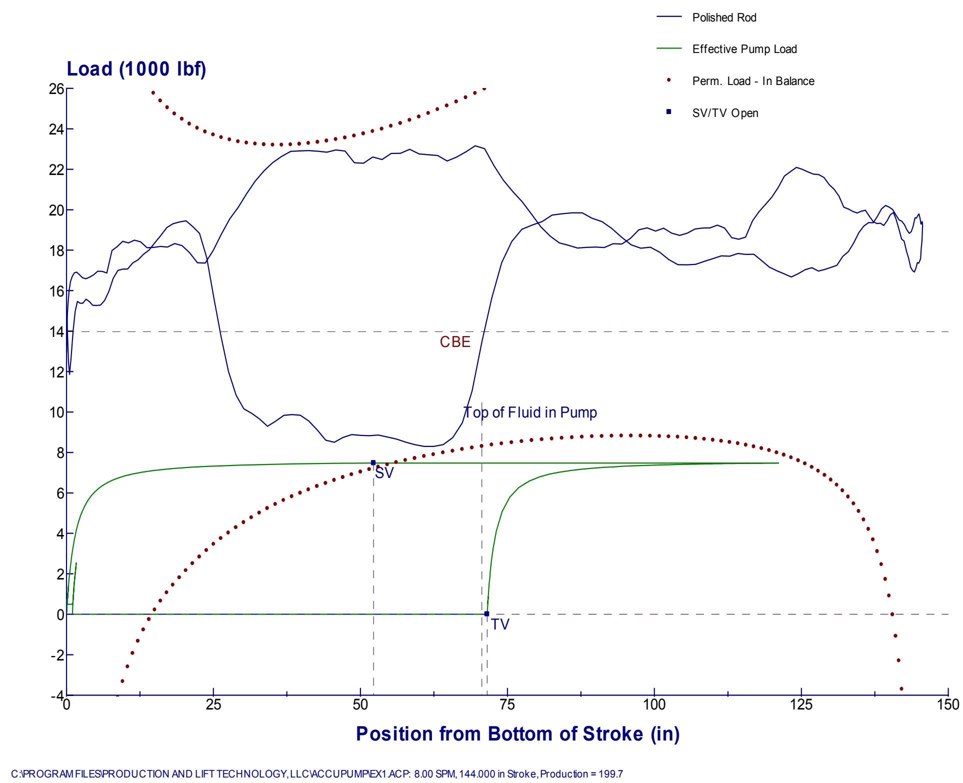

Figure 6a - Calculate Pump Cards for 60% Pump Fillage

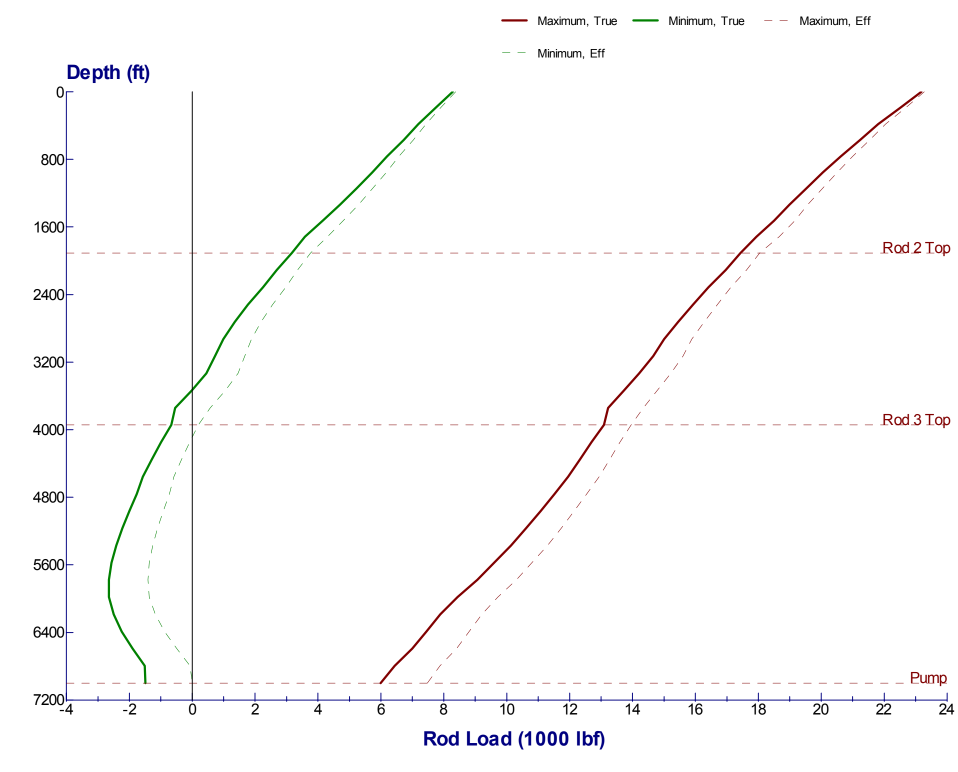

Figure 6b - Rod Loads for 60% Pump Fillage

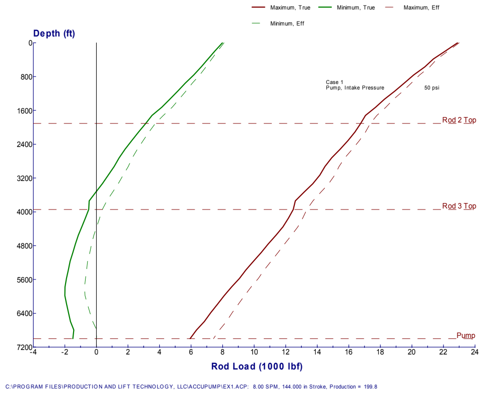

Intake Pressure = 50 psi

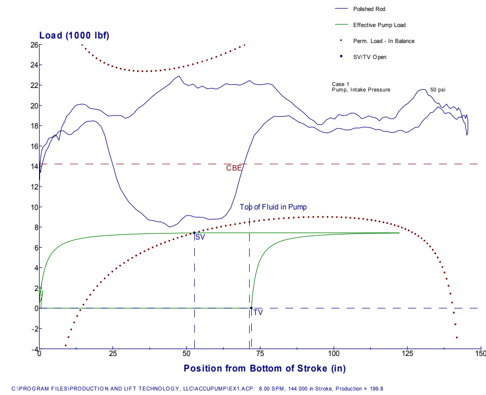

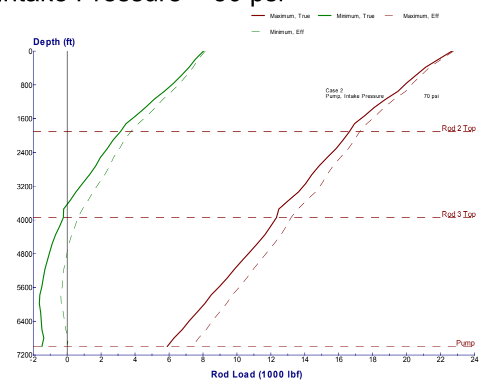

Intake Pressure = 70 psi

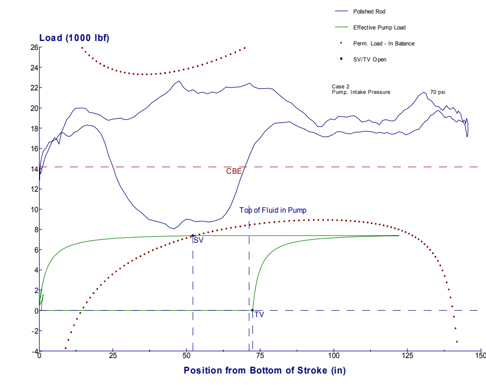

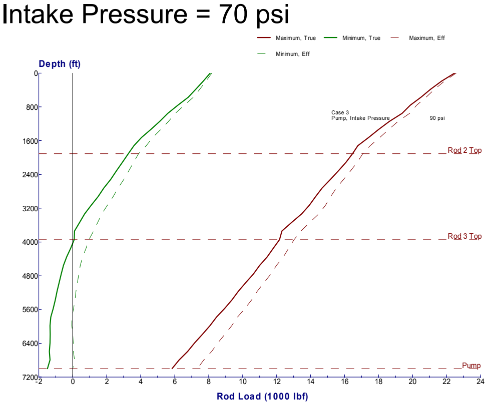

Intake Pressure = 90 psi

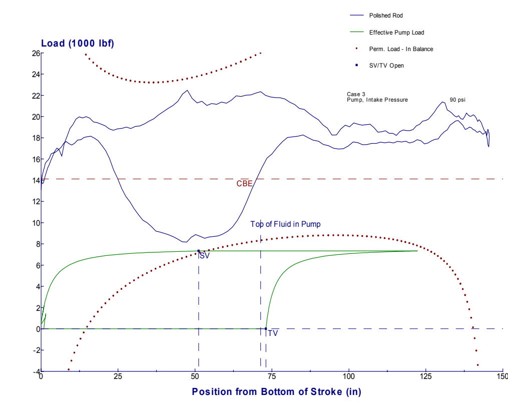

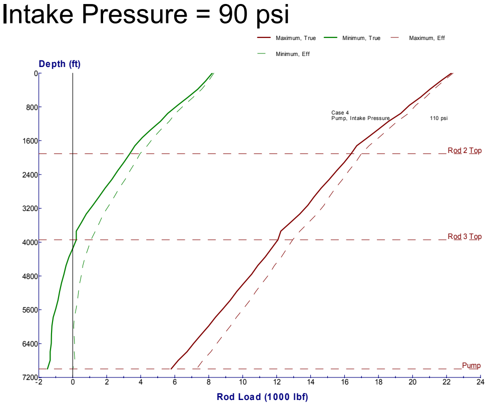

Intake Pressure = 110 psi

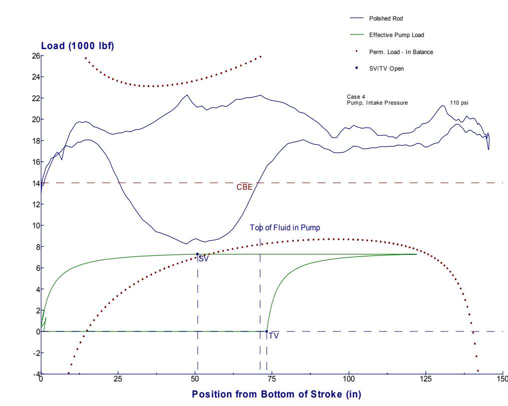

Figure 7 - Vary Intake Pressure. Pump Fillage = 60%, 8 spm

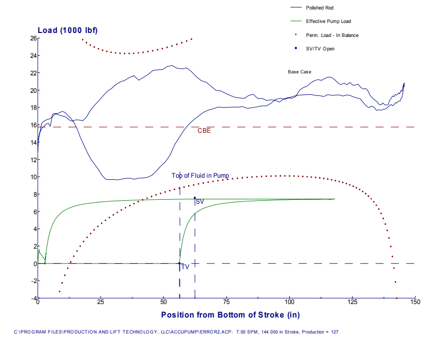

Pump Fill = 50%

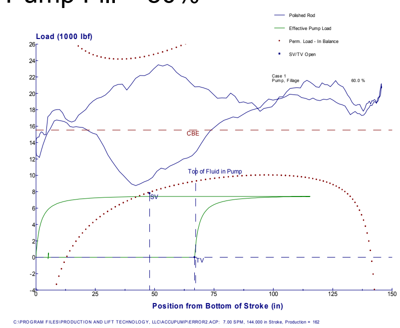

Pump Fill = 60%

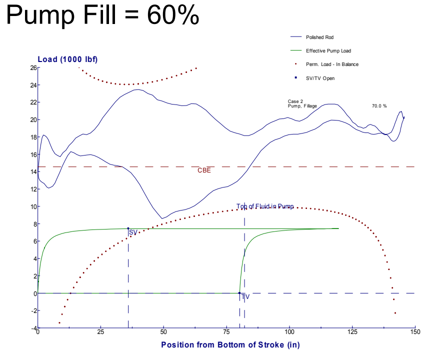

Pump Fill = 70%

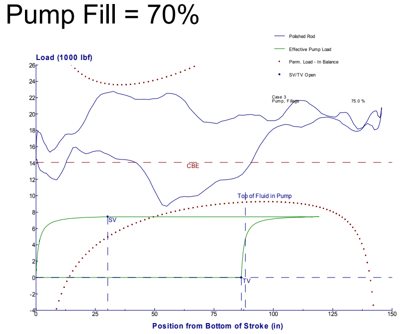

Pump Fill = 80%

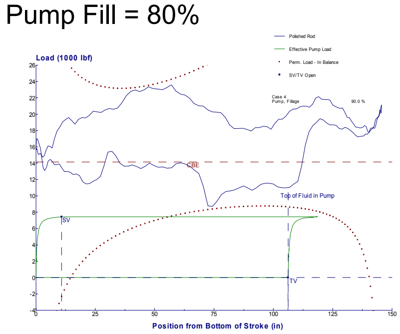

Pump Fill = 90%

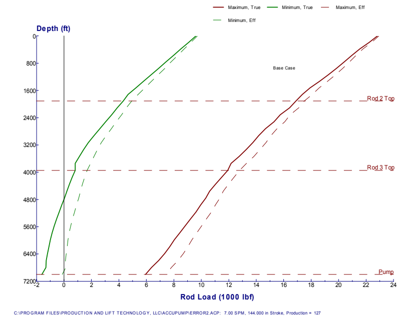

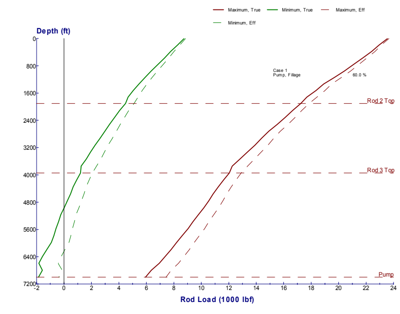

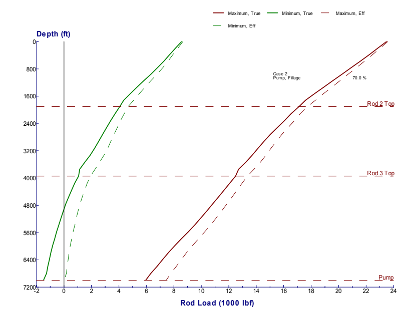

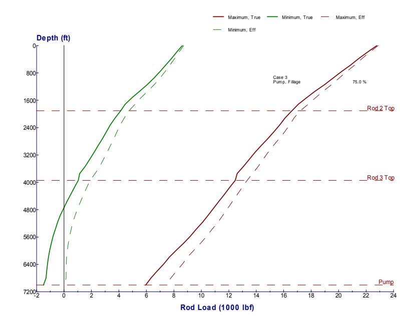

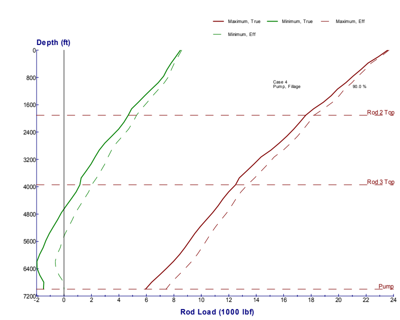

Figure 8 - Vary Fillage, Intake Pressure = 50 psi,7 spm

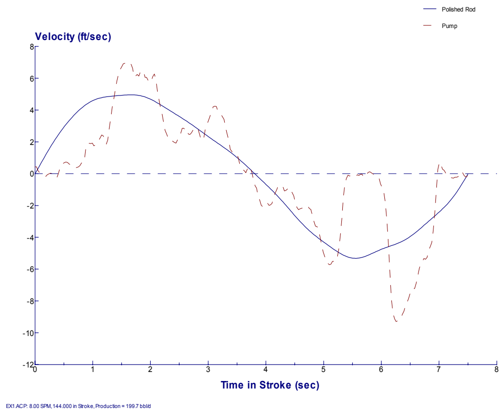

Figure 9 - Pump and Surface Velocity in a Pump Cycle

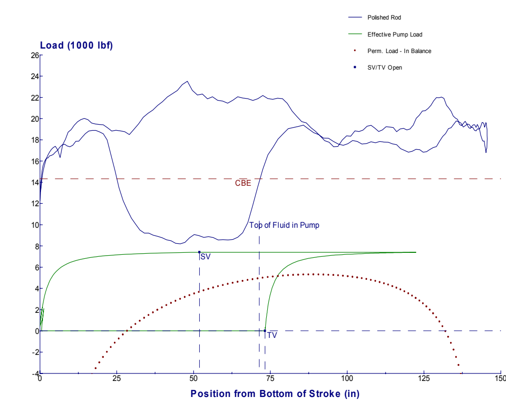

(a)

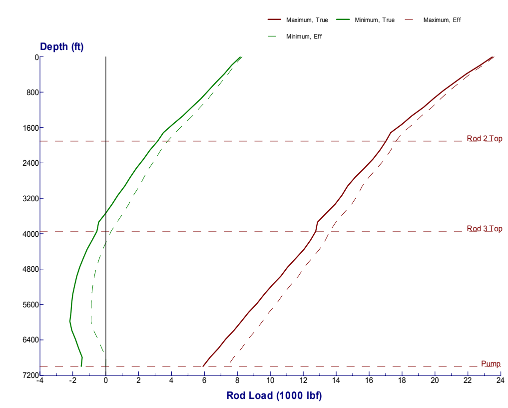

(b)

8 spm, 60% fillage, 86 rod string

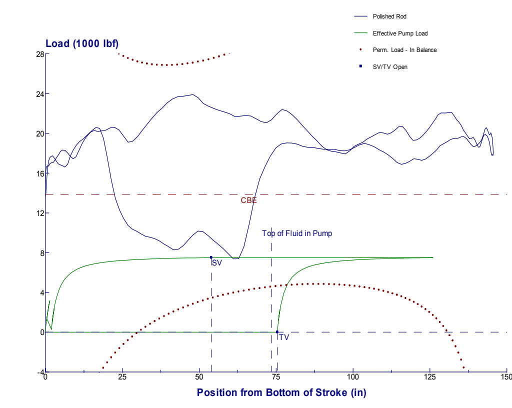

(c)

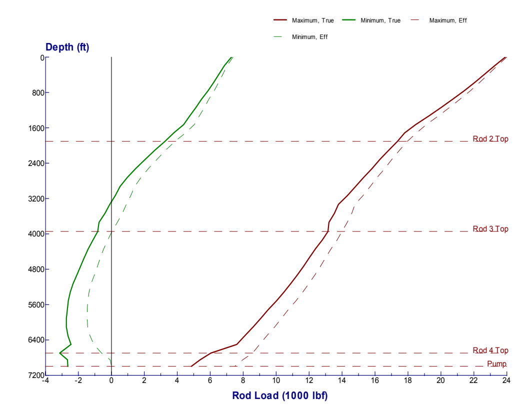

(d)

8 spm, 60% fillage, 86 rod string with 300 feet of 1” sinker bars

Figure 10 - Effect of Sinker Bars